Journal of Materials Chemistry C

Accepted Manuscript

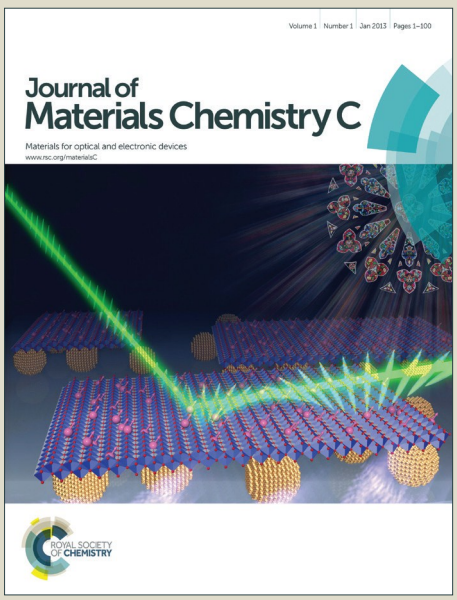

ROYAL SOCIETY OF CHEMISTRY

www.rsc.org/materialsC

Journal Name

ARTICLE

Unique "Cage-Cage" Shaped Hydrophobic Fluoropolymer Film Derived from Novel Double-Decker Structural POSS with Low Dielectric constant

Received 00th January 20xx,
Accepted 00th January 20xx

DOI: 10.1039/x0xx00000x

www.rsc.org/

Qiyang Jiang, Weihai Zhang, Jinmeng Hao, Yanfeng Wei, Jianxin Mu*, Zhenhua Jiang

This work focuses on the design of unique "cage-cage" shaped low dielectric constant and hydrophobic materials with nano-sized pores and least polarizable groups existing. Therefore, a novel double-decker structural fluorinated POSS was first synthesized, which then reacted with diphenol POSS to produce the linear hybrid polymers. When the merits of fluoride and nanoporous structure are combined, the dielectric constant of the hybrid material decreases significantly (2.24 at 1 MHz) along with the low surface energy (contact angle of 107° in water) of the material, as well as good solubility and thermal properties.

Introduction

Materials with low dielectric constant (κ value) have recently attracted much attention as solutions to resistance-capacitance delays, signal crosstalk, and power consumption in integrated circuits (ICs).[1-3] Traditional materials with low dielectric constant cannot meet the requirements of IC application, and although many alternatives have been explored, novel materials with low dielectric constant, low dielectric loss (low tan δ), and other excellent properties are difficult to identify for use in future devices. The surface hydrophobicity of films is a crucial factor in reducing the environmental sensitivity of materials, hydrophobic materials can maintain an insensitive dielectric constant in different environments.[4] Hence, materials must be developed with low dielectric constant and hydrophobic surfaces.

Recent studies report two promising approaches for developing low-dielectric materials.[5] A common approach involves the addition of least polarizable groups (e.g., C-H, C-Si, C-F) to polymer matrices to reduce material polarizability. Another approach involves introducing nanopores into films to increase pore density. With this increase, the polarizability and κ value of materials can decrease significantly. Fluoropolymers are potential candidates for IC application because they show lower κ values and excellent hydrophobic properties.[6,7] However, it is limited to reduce the dielectric constant of the materials just by introducing lower molecular polarizability fluorine element. To fabricate hydrophobic materials with low κ dielectric constants, we utilized novel fluoro-polyhedral oligomeric silsesquioxanes (POSS) in the current study. This material has low polarizability and low levels of free energy. Moreover, it can generate nanopores in materials to prepare hydrophobic materials with low dielectric constant.

POSS is a family of nanometer-sized silicon-oxygen cage structures (Si_8O_{12}). Each apex (silicon atom) is connected to organic groups.[8-10] The unique cage structure of POSS can construct nanopores in polymers. The reactive POSS molecules can be incorporated into polymers to form dendronized, grafted conjugated, or main chain-shaped hybrid polymers, depending on the number of POSS functional groups.[11-15] Linear hybrid polymers with POSS in the main chain are advantageous in the following ways over grafted and cross-linked POSS-containing hybrid polymers: the flexible adjustability of the chemical structure, excellent solubility, and molecular chain regularity. Masa-aki Kakimoto et al.[16] who summarize synthesis of low dielectric constant polyimides containing novel difunctional POSS in the main chain and polymers exhibited the lowest dielectric constant (2.43 at 1 MHz). Lee et al.[17] reported the preparation of POSS-based hybrids with network structure, the lowest dielectric constant was 2.65. More recently, Hongyao Xu et al.[18] reported the synthesis of hybrids with different architectures including dumbbell-type, bead-type, and cross-linked structure via the Heck reaction between octavinyl-polyhedral oligomeric silsesquioxane (OV-POSS) and different bromo-substituted aromatic amide monomers. The POSS-based hybrids exhibited good thermal stability and low dielectric constant properties. However, this works doesn't focus on the low dielectric constant properties and hydrophobic surfaces, Therefore, it is of interest to synthesis linear hybrid polymers with POSS in the main chain with lower dielectric constant properties, especially there has been no previous reports for the synthesis of main chain POSS at high levels.

College of Chemistry, The Key Lab of High Performance Plastics, Ministry of Education, Jilin University, Changchun 130012, P. R. China
E-mail: jianxin_mu@jlu.edu.cn;
Fax: 86-431-88498137; Tel:86-431-88498137.

The key to obtaining linear hybrid polymers with POSS at high levels is the synthesis of two functionalized, highly active POSS-containing monomers. In addition, to ensure that all the polymerization monomers containing POSS groups is another important issue to ensure the content of POSS in linear hybrid polymers. Double-decker-shaped silsesquioxane (DDSQ) possesses two reactive hydrosilane groups and is considered a promising monomer for synthesizing linear hybrid polymers containing POSS in the main chain.[19-22] Thus, double-decker structural fluorinated POSS (10F-DDSQ) and diphenol POSS (2OH-DDSQ) are synthesized in the current study to prepare linear "cage-cage" shaped hydrophobic hybrid polymers containing high level POSS nanoporous with low dielectric constant.

The "cage–cage" shaped polymer in this study is a new example to obtain the low dielectric constant materials by introducing large amount of nanopores POSS in the main chain of polymers. When the merits of fluoride and nanoporous structure are combined, the polarizability of the hybrid material decreases significantly along with the surface energy of the material. Furthermore, the synergistic effects of fluorine and POSS on the dielectric constant and on the hydrophobic properties of polymer are studied systematically.

Experimental Section

Materials

All chemicals and solvent are of reagent grade unless otherwise indicated. Triethylamine, 1-Methyl-2-pyrrolidinone (Aladdin), N,N-dimeth-ylacetamide (Aladdin), and toluene were distilled over CaH_2. Tetrahydrofuran (THF) was distilled over sodium. Eugenol (Aladdin) was purified through vacuum distillation over CaH_2 prior to use. Phenyltrimethoxysilane (Energy-Chemical), potassium carbonate, allylpentafluorobenzene (Aldrich), and other solvents were used without further purification.

Instruments

^1H and ^{13}C NMR spectra were performed with a Brüker Advance 300 spectrometer (300 MHz) in $CDCl_3$. ^{19}F NMR, and ^{29}Si NMR measurements were conducted using a Brüker 510 NMR spectrometer (500 MHz) in $CDCl_3$. ^{29}Si MAS NMR measurements were performed with a Brüker Avance NMR spectrometer (500 MHz) equipped with a 4-mm MAS probehead. Fourier transform infrared (FTIR) spectra were obtained using a Nicolet Impact 410 FTIR spectrophotometer. An experiment was conducted with matrix-assisted laser desorption/ionization time-of-flight mass spectroscopy (MALDI-TOF-MS) using a Shimadzu/AMIMA-CFR. Gel permeation chromatography (GPC) was performed using a Waters 410 instrument with dimethylformamide as an eluent and polystyrene as the standard. Thermogravimetric analysis (TGA) and differential scanning calorimetry (DSC) were conducted using a PerkinElmer Pryis 1 TGA analyzer and a Mettler-Toledo Instrument DSC 821^e-modulated thermal analyzer with a heating rate of 10 ^oC/min under air and nitrogen. Dielectric constants were measured by a Hewlett–Packard 4285A precision impedance analyzer at frequencies ranging from 10^3 Hz to 10^6 Hz. Contact angles were determined with a POWEREACH/JC2002C2 contact angle meter at room temperature. The crystallization behavior of the hybrid polymer and the control PAES were examined using a Rigaku D/max-2500 X-ray diffractometer with Cu Ka radiation (λ = 0.154 nm) as the X-ray source. Topographical and lateral atomic force microscopy (AFM) images were obtained using SPA300 Discoverer scanning probe microscope. The dispersion of POSS clusters in the polymer matrix was observed using FEI Nova NanoSEM 450 microscope. The Transmission electron microscope (TEM) images were collected on a JEM-3010 transmission electron microscope (spherical aberration constant C_s=0.6mm) operated at 300 kv and were recorded by a bottom-mounted CCD camera (Gatan MultiScan Camera Model 794).

Synthesis of macromers

Compound 3,13-di(2-methoxy-4-propylphenol)octaphenyl DDSQ was synthesized by following a reported procedure.[23] 3,13-di(1,2,3,4,5-pentafluoro-6-propylbenzene)octaphenyl DDSQ (10F-DDSQ) was synthesized by hydrosilylation reaction between 3,13-dihydrooctaphenylhexacyclodecasiloxane (dihydro-DDSQ) and allylpentafluorobenzene that was catalyzed by Karstedt's catalyst, as shown in Scheme 1. As in a typical procedure, a 100-ml two-necked, round-bottomed flask was equipped with a magnetic stirrer, a nitrogen inlet, and an anhydrous calcium chloride drying tube. This flask was connected to a Schlenk line for degassing by a repeated exhausting-refilling process using pure nitrogen. Dihydro-DDSQ (2.3 g, 2 mmol), allylpentafluorobenzene (0.87 g, 4.2 mmol), and toluene (20 ml) were then added to the flask. The reaction product obtained with 30 min of vigorous stirring was catalyzed by Karstedt's catalyst [Pt (dvs)] (5 drops, 0.2 mol %) in toluene at 95 ^oC for 24 h and then held for 12 h at 105 ^oC with stirring to ensure that the hydrosilylation process was completed. The solvent and excess allylpentafluorobenzene were removed under reduced pressure to yield almost-colorless solids (2.85 g, yield: 91%). ^1H-NMR (300 MHz, $CDCl_3$, δ): 7.1 to 7.74 (m, 40H), 2.61 (t, J = 7.2 Hz, 4H; $SiCH_2CH_2CH_2$-), 1.67 (t, J = 7.5 Hz, 4H; $SiCH_2CH_2$-), 0.75 (t, J = 8.1 Hz, 4H; $SiCH_2$-), and 0.30 (s, 6H, Si-CH_3); ^{13}C-NMR (300 MHz, $CDCl_3$, δ): 15.63, 22.13, 24.73, 112.32, 128.04, 129.94, 130.95, and 133.18; ^{19}F-NMR (500 MHz, $CDCl_3$, δ): -144.17, -156.15 and -163.01; MALDI-TOF-MS m/z (%): 1571.70 (29) $[M^+]$, 1593.87 (100) $[M+Na]^+$.

Synthesis of Polymer

As in a typical experiment (Scheme 1), 2OH-DDSQ (1.48 g, 1 mmol), K_2CO_3 (0.17 g, 1 mmol), NMP (9.2 ml), and toluene (4.6 ml) were added to a 25-ml three-necked flask equipped with a mechanical stirrer, a nitrogen inlet, and a Dean-Stark trap with a condenser. The reaction mixture was heated to 170 ^oC to 180 ^oC, and this temperature was maintained for 12 h to ensure complete dehydration. The benzene was refluxed into the Dean-Stark trap. Upon removing the benzene, the reaction

mixture was cooled to 60 °C. Then, 10F-DDSQ was added. The temperature was maintained for 12 h to complete the polymerization reaction. The viscosity of the solution noticeably increased after 12 h. Subsequently, this solution was poured into distilled water. The precipitate was filtered off, washed several times with water and ethanol to remove the salts and solvents, and then dried at 120 °C for 24 h to stabilize weight. The yield was 92%. GPC (dimethylformamide) M_n : 22779 g/mol, M_w: 39540 g/mol; ^{1}H-NMR (300 MHz, $CDCl_3$, δ): 6.64 to 7.9 (m, 40H, Ar H of Si-Ph), 6.32 to 6.63 (m, 3H, Ar H), 3.64 (s, 6H, CH_3-O), 2.45 (br, 4H, $SiCH_2CH_2CH_2$-), 1.54 (br, 4H, $SiCH_2CH_2$-), 0.62 (br, 4H, $SiCH_2$-), and 0.30 (s, 6H, Si-CH_3); ^{29}Si-MAS NMR (500 MHz, δ): -19.97, -66.83, and -80.73. ^{19}F-NMR (500 MHz, $CDCl_3$, δ): -145.17 and -156.97.

Results and discussion

Surface Properties of polymer

The surface hydrophobicity of polymer is examined by measuring contact angles. The contact angle of the static surface is measured with water as probe liquid. This angle is determined on polymer coating prepared from N, N-dimethylacetamide (DMAc) solution that is spin casted onto glass. The contact angle of polymer in water is greater than 107°.

On the one hand, the relationship between the contact angle and surface energy is governed by Wenzel equationas (Equation (1)). Where θ_w is the equilibrium contact angle, γ^{sa}, γ^{sl}, γ^{la} are solid-gas, solid-liquid and liquid-gas interfacial tension, γ is roughness factor of solid surface. For hydrophobic surface, contact angle increased with increasing the roughness of materials. Surface roughness improves the surface hydrophobicity of polymers. Fig. 1 shows the surface of the polymer generated through AFM. The average surface roughness measured is 7.25 nm, which indicates a rougher film surface than the majority of fluoropolymer films, it is noted that the surface roughness acts as a crucial agent to the hydrophobicity of film. This roughness corresponds to the film uniformity that can meet the requirements of the low-κ materials utilized in IC.

$$\cos\theta_w = \gamma \times \frac{\left(\gamma^{sa} - \gamma^{sl}\right)}{\gamma^{la}} = \gamma \cos\theta_Y$$

On the other hand, the surface free energy of the film is 10.24 m N m^{-1}, indicating of which the DDSQ cages with low surface energy and fluorine atoms can minimize the surface energy of hybrid materials.

Dielectric Constant of Film

Fig. 2 presents the κ value of the polymer, which is only 2.24. Furthermore, dielectric loss is less than 1.92×e^{-3} at 1 MHz. This loss is considerably lower than that of traditional materials under the same test condition.

The reason why the polymer exhibited excellent dielectric properties can be explained by the equations below.

On the one hand, POSS contains a well-defined, nanoscale inorganic core that generates a large quantity of nanopores in materials (Fig. 3). The SEM of thin-film sections revealed a homogeneous distribution of POSS in the polymer, and depict a continuous phase which incorporates these nanosized POSS at a molecular level. Porous films are usually regarded as hybrid materials that are composed of a solid phase and holes; this phase shares a dielectric constant κ_2 with dense materials.

Moreover, the dielectric constant κ_r of porous films is determined on the basis of porosity. κ_1 = 1 when the holes are filled with air, as calculated using Equation (2).

$$\frac{\kappa_r - 1}{\kappa_r + 2} = \frac{4}{3}\pi N\left(\alpha_e + \alpha_d + \frac{\mu^2}{3\kappa_b T}\right)$$

This equation indicates that the dielectric constant of polymer decreases as the porosity of films increases.

On the other hand, this finding can be explained by the Debye equation (Equation (3)), where κ_r is the dielectric constant, N is the number density of dipoles, α_e is electric polarization, α_d is distortion polarization, μ is the orientation polarization related to the dipole moment, κ_b is the Boltzmann constant, and T is temperature. For polymer, the incorporation of C-F bonds made the molecule difficult to be polarized, resulting in the reduction of α_e. Moreover, the introduction of the bulky and vacant cage-like structure of the POSS macromers resulted in the polymer chains unable to undo chain entanglements in the main chains of the copolymers, thereby diminishing N. The μ value of amorphous structure is generally small given the low anisotropy. Thus, the reduction of N, μ, and α_e results in low dielectric constants for polymers.

$$\frac{\kappa_r - 1}{\kappa_r + 2} = p \cdot \frac{(\kappa_1 - 1)}{(\kappa_1 + 2)} + (1 - p) \cdot \frac{(\kappa_2 - 1)}{(\kappa_2 + 2)}$$

Moreover, the interlayer distance of the polymers shown in Fig. 4 may be related to the X-ray diffraction (XRD) peak at 2θ = 7.3° (d = 1.21 nm), as shown in Fig. 5. A significant interlayer distance may lower polymer density. This decrease may contribute to a low dielectric constant.

In summary, the synergistic effect of POSS and fluorine generates a low dielectric constant.

The low dielectric property of polymer remains stable for over 14 days in a clean room under ambient conditions (23 °C, humidity level of 50%), as illustrated in Fig. 6. The value of this property increases only slightly by 0.09 or 4%. The stable dielectric constant of the film can be attributed to the steady hydrophobic property.

Thermal Properties of polymer

Thermal properties are excellent because of the $Si_{10}O_{14}$ cage structure. The thermal stability of the hybrid materials is evaluated through TGA. In fact, the TGA curve is exhibited in Fig 7. The polymer lost 5% weight at 428 °C. The polymer degradation process involves two steps: the first begins with the degradation of the active alkyl chain, and the second starts with the degradation of frameworks, such as aromatic rings and POSS cages. The hybrid material experienced high residual

degradation at 42%. The degradation residue yields are ascribed to the silica formation from POSS moieties during thermal decomposition. DSC is conducted to measure the T_g value of the hybrid material. This value is 163 °C of the polymer and is affected by two opposite tendencies. The nanoreinforcement of POSS cages in the main chains significantly enhances the rigidity of the main chains, thereby restricting the motion of polymer chains. This restriction enhances T_g. On the contrary, the bulky, vacant, cage-like Si-O-Si structure of POSS macromers increases the free volume of the chains. As a result, the polymer chains cannot be packed densely in glassy state. As a consequence, the T_g of the polymer decreases. In the present case, the nanoreinforcement of DDSQ in the main chains dominates the effect on glass transition temperature.

The solubility of the hybrid polymer

The solubility of the polymer is investigated as well. The result shows that the polymer can be dissolved effectively in various common organic solvents, such as DMAc, chloroform, tetrahydrofuran, and 1-Methyl-2-pyrrolidinone (NMP) at room temperature.

Conclusions

In conclusion, to the best of our knowledge, unique "cage-cage" shaped hydrophobic fluoropolymer films with low dielectric constant derived from novel double-decker structural fluorinated POSS and diphenol POSS was prepared successfully via nucleophilic aromatic substitution. The novel double-decker structural POSS-containing monomers pave a promising method for synthesizing linear hybrid polymers with POSS in the main chain at high levels. The novel "cage-cage" shaped polymers can also facilitate the production of hydrophobic, high-performance materials with low dielectric constant. Such material has a low κ value of 2.24 at 1 MHz and a high contact angle of 107° in water, as well as good solubility and excellent thermal properties. Given its unique structure, this type of polymer is a good candidate for polymeric material against advanced materials with low dielectric constant, highly-used temperature composites, or surface-modified supports.

Acknowledgements

The authors gratefully acknowledge the financial support from the International Science and Technology Cooperation program of China (2012DFR50300).

Notes and references

1 M. Ree, J. Yoon and K. Heo, J, *Mater. Chem*., 2006, **16**, 685.
2 R. Q. Su, T. E. Muller, J. Prochazka and J. A. Lercher, *Adv. Mater*., 2002, **14**, 1369.
3 R. D. Miller, *Science*, 1999, **286**, 421.
4 C. M. Yang, A. T. Cho, F. M. Pan, T. G. Tsai and K. J. Chao, A*dv. Mater.,* 2001, **13**, 1099.
5 C. Leu, G. M. Reddy, K. Wei and C. Shu, *Chem. Mater*. 2003, **15**, 2261.
6 G. Maier, *Prog. Polym. Sci.,* 2001, **26**, 3.
7 S.T. Iacono, A. Vij, W. Grabow, D.W. Smith and J.M. Mabry, *Chem. Commun*., 2007, 4992.
8 E. Sacher, *Prog. Surf. Sci.,* 1994, **47**, 273.
9 J. D. Lichtenhan, *Comments. Inorg. Chem*., 1995, **17**, 115.
10 G. Li, L. Wang, H. Ni, C. U. Pittman and J. Jr. *Organomet. Polym.,* 2001, **11**, 123.
11 E. Markovic, S. Clarke, J. Matisons, G. P. Simon, *Macromolecules*, 2008, **41**, 1685
12 C. Zhao, X. Yang, X. Wu, X. Liu, X. Wang and L. Lu, *Polym. Bull.,* 2008, **60**, 495
13 J. Wu and P. T. Mather, *J. Macromol. Sci., Polym. Rev.,* 2009, **49**, 25.
14 B. X. Fu, B. S. Hsiao, H. White, M. Rafailovich, P. T. Mather, H. G. Jeon, S. Phillips, J. D. Lichtenhan and J. Schwab, *Polym. Int.,* 2000, **49**, 437.
15 A. J. Waddon and E. B. Coughlin, *Chem. Mater.,* 2003, **15**, 4555.
16 S. Wu, T. Hayakawa, M.-A. Kakimoto and H. Oikawa, Macromolecules, 2008, **41**, 3481.
17 Y. J. Lee, J. M. Huang, S. W. Kuo, J. S. Lu and F. C. Chang, Polymer, 2005, **46**, 173.
18 18.F. Y. Ke, C. Zhang, S. Y. Guang, H. Y. Xu and N. B. Lin, J. Appl. Polym. Sci., 2015, 42292.
19 M. Seino, T. Hayakawa, Y. Ishida, M. Kakimoto, K. Watanabe and H. Oikawa, *Macromolecules,* 2006, **39**, 3473.
20 S. T. Iacono, A. Vij, W. Grabow, D. W. Smith and J. M. Mabry, *Chem. Commun.,* 2007, 4992.
21 L. Zheng, S. Hong, G. Cardoen, E. Burgaz, S. P. Gido and E. B. Coughlin, *Macromolecules*, 2004, **37**, 8606; B.-Y. Kim and P. T. Mather, *Macromolecules*, 2002, **35**, 8378.
22 K. Yoshida, K. Ito, H. Oikawa, M. Yamahiro, Y. Morimoto, K. Ohguma, K. Watanabe and N. Ootake, United States Patent Application 20040249103A1.
23 W. H. Zhang, J. D. Xu, X. S. Li, G. H. Song, J. X. Mu, *J. Polym. Sci., Part A: Polym. Chem.,* 2014, **52**, 780.

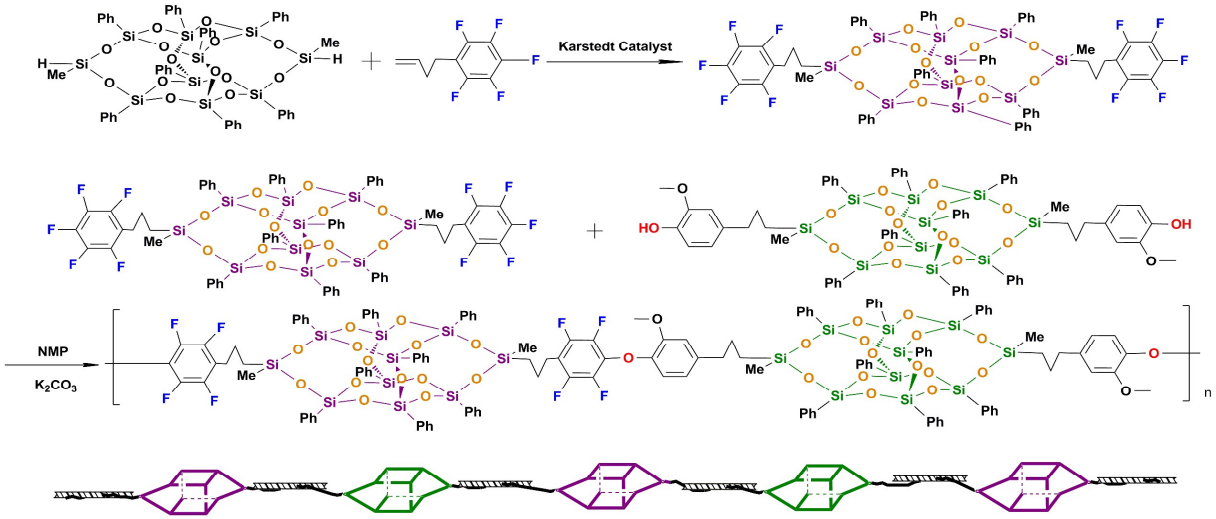

Scheme 1 Synthetic route to 10F-DDSQ and Polymer.

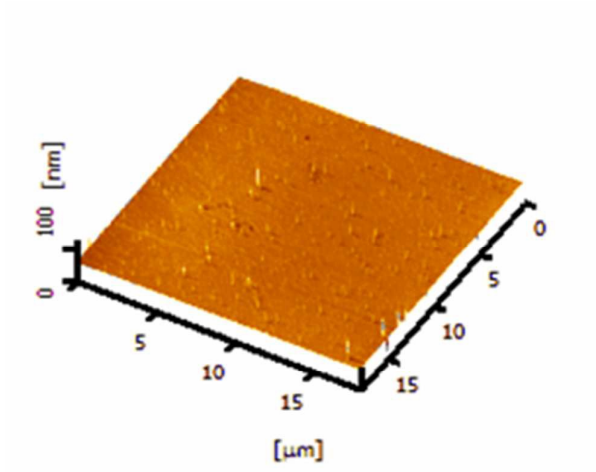

Fig. 1 AFM image of the film on glass.

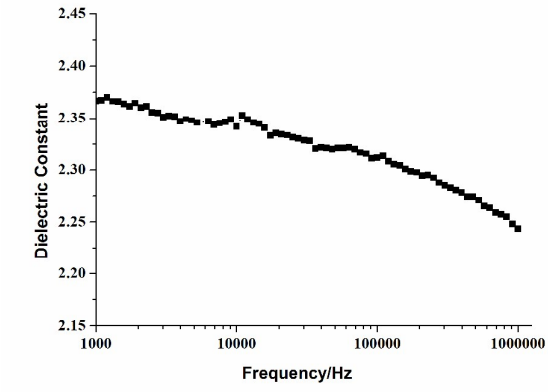

Fig. 2 Frequency dependence of the dielectric constants of the synthesized polymer.

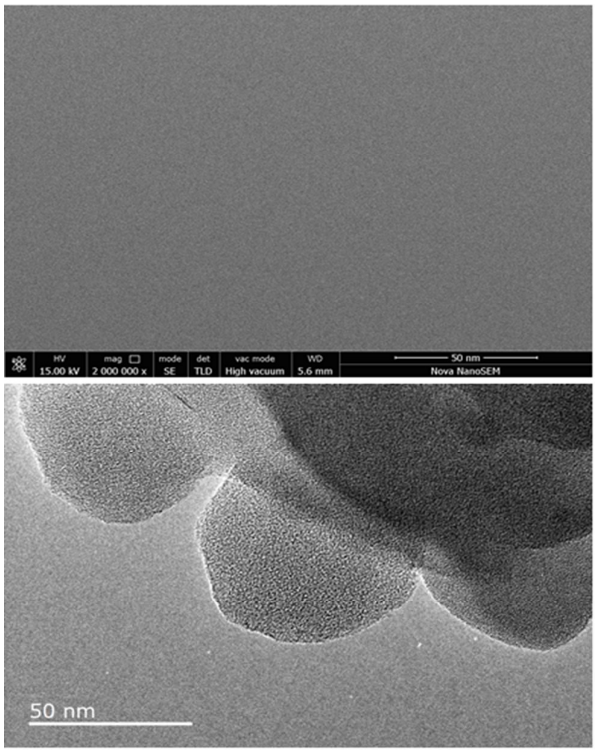

Fig. 3 SEM and TEM images of polymer

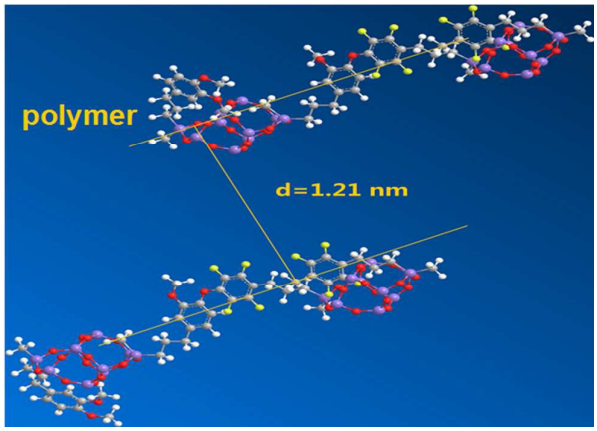

Fig. 4 Postulated solid structure of the synthesized polymer. The average interlayer distance was 1.21 nm, as calculated from XRD data.

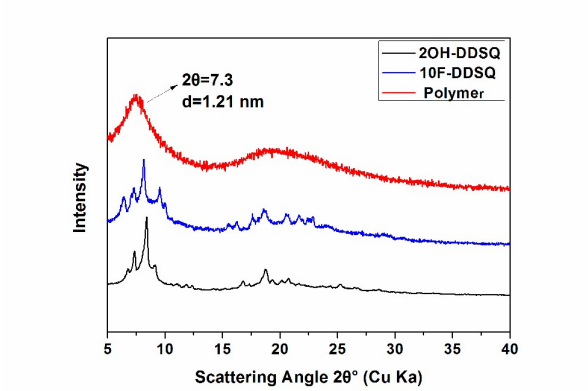

Fig. 5 XRD patterns of the synthesized polymer in powder.

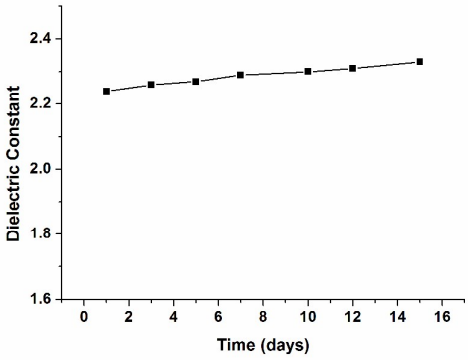

Fig. 6 Dielectric constant of the film as a function of storage time in a clean room under ambient conditions.

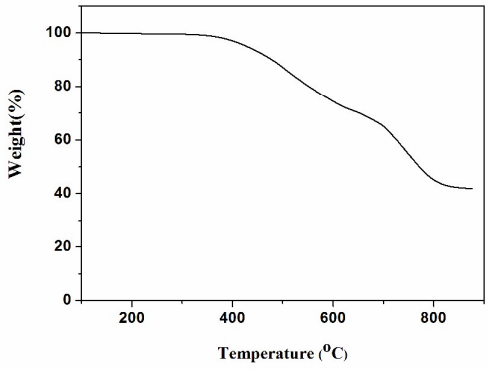

Fig. 7. TGA curve of the synthesized polymer in air with a heating rate of 10 °C/min.

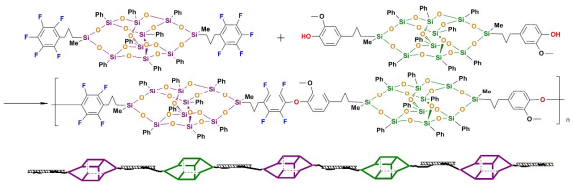

Novel double-decker structural fluorinated POSS and diphenol POSS were first synthesized for preparing a unique “cage-cage” -shaped hydrophobic fluoropolymer film with an ultra-low dielectric constant.